

TE Coolers Computer Simulation: Incremental Upgrading of Rate Equations Approach

D. Kondratiev, L. Yershova
RMT Ltd. 53 Leninskij prosp. Moscow 119991 Russia
phone: 095-132-6817 fax: 095-132-5870
e-mail: rmtcom@dol.ru <http://www.rmtltd.ru>

Abstract

Thermoelectric (TE) technique and TE Cooler (TEC) exposure becoming more and more involved, both a manufacturer and a user are facing the problem of modeling and characterizing TEC mathematically. We suggest one of the approaches to do it based on (quasi-) tri-diagonal rate matrix of rate equations describing one-dimensional thermal dynamics through all intermediate stages and layers, including ceramics and solders, as well as a possible housing and temperature dependence of the parameters.

Introduction

Either in TEC developing or constructing, in TEC controlling or testing one has to deal with the proper mathematical and, nowadays, computer aid. The problems of vital concern are the following:

- Mathematical modeling prior to technical development and constructing
- Selecting a suitable TEC from a variety
- TEC operation modeling in real conditions

This problem has already been considered and touched upon in a number of papers^{1,2,3} and others.

We suggest one of the approaches to do it supported by the software program TECcad. The approach is based on the set of rate equations describing one-dimensional thermal dynamics through all intermediate stages and layers, including ceramics and soldering.

In the simplest case describing TEC means solving a set of temperature linear rate equations. We consider this rate equations should be well adjusted for simulating an N-stage TEC (N can be of any value), allowing for a finite thermal conductance of insulating and metal participants, thermal exchange through leading wires, air and radiation.

This paper goal is to offer a possible step-by-step approach for solving the two-way problem: Cooling parameters ↔ TEC structure.

The architecture of the approach is defined by increments.

Sections 1 and 2 proceed from modeling one-stage TEC's to N-stage ones where N is selectable. The problem of these sections is limited to the simplest case: no radiation, no air conductance between the TEC legs and no heat sink, or cap, no parameters thermal dependence. Section 3 solves the problem of allowing for temperature dependence of thermoelectric parameters. Section 4 eliminates the limits of the previous sections allowing for radiation, air conductance between the TEC legs, heat sink and/or cap. Section 5 applies the theory developed in Sec. 1-4 to the problem of maximum and optimal TEC operation modes. In conclusion we describe all the above results as the grounding of computer simulation, optimal selection and constructor-aiding program TECcad.

1. Single-stage TEC

In the simplest case to describe a TE cooler operation means to solve a set of rate temperature linear equations. First consider a one-stage TE cooler with n pellets. In Fig. 1.1 you see such a cooler model with junctions temperatures marked.

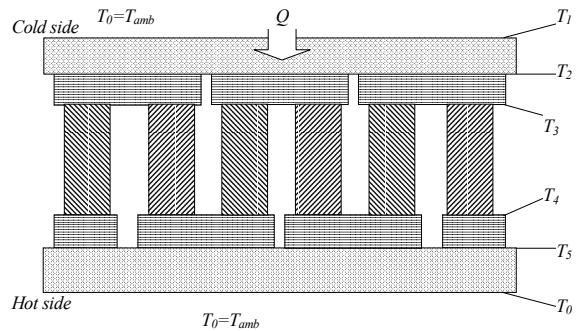


Fig.1.1. Temperature distribution in a one-stage TE cooler

The set of equations describing this model is like this:

$$\begin{aligned}
 k_0 (T_0 - T_1) - k_{c_0} (T_1 - T_2) + Q &= 0 \\
 k_{c_0} (T_1 - T_2) - k_{me} (T_2 - T_3) \frac{n}{2} &= 0 \\
 n \left(\alpha T_3 - \frac{1}{2} I^2 (R + r/2) + k_{me} \frac{1}{2} (T_2 - T_3) \right) &= 0 \\
 n \left(\alpha T_4 + \frac{1}{2} I^2 (R + r/2) - k (T_4 - T_3) - k_{me} \frac{1}{2} (T_4 - T_3) \right) &= 0 \\
 k_{me} \frac{n}{2} (T_4 - T_5) - k_{c_1} (T_5 - T_0) &= 0
 \end{aligned} \tag{1.1}$$

where $k_0 = aS_0$, a is heat conduction value from the upper ceramics surface S_0 ; $k_{me} = \kappa_{me} \frac{(2x+d)x}{l_{me}}$ is metal junction thermal conductivity; κ_{me} is metal junction specific thermal conductivity; l_{me} is metal junction width, x is a pellet width, d is the distance between pellets. We took into account, that the metal junctions number on each surface is $n/2$. $k_{c_i} = \kappa_c \frac{S_i}{l_c}$ is ceramics thermal conductivity; κ_c is ceramics specific thermal conductivity; S_i , l_c is ceramics footprint area and width respectively; $i=0$ is referred to the upper ceramics; $i=1$ is to the lower one; R, r are resistance values of a pellet and metal junction, $R = \rho \frac{l}{s}$, $r = \rho_{me} \frac{d + (2/3)x}{l_{me} \times x}$; ρ, ρ_{me} - corresponding specific resistances; s is pellet cross-section, S is the corresponding stage cold side area.

The first equation in the set is present independently of the number of stages. The other four characterize the stage itself. The matrix view is more convenient for computer simulation. It is given in Appendix A1.

2. Multi-stage TE Cooler Mathematical Modeling

Let us consider the general case of an N-stage Peltier module. This case schematically is presented in Fig. 2.1.

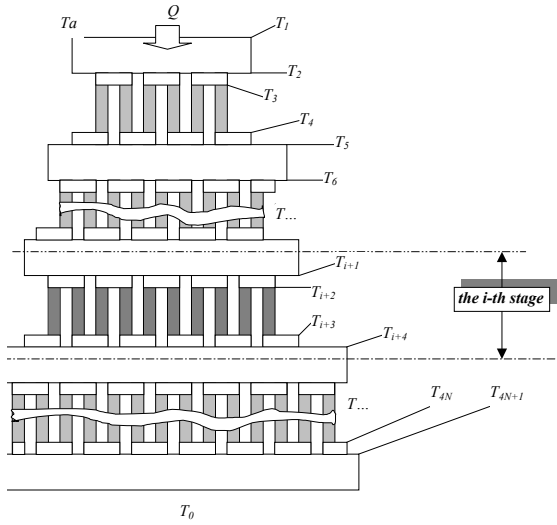


Figure 2.1. A multi-stage TEC structure with all the intermediate temperature values.

N-stage TE cooler involves a set of $4N+1$ equations (2.1).

$$\begin{aligned}
 & k_0(T_0 - T_1) - k_{c0}(T_1 - T_2) + Q = 0 \\
 & k_{c0}(T_1 - T_2) - k_{me} \frac{n_1}{2}(T_2 - T_3) = 0 \\
 & n_1 \left(-\alpha T_3 + \frac{1}{2} I^2 (R+r/2) + k(T_4 - T_3) + k_{me} \frac{1}{2}(T_2 - T_3) \right) = 0 \\
 & n_1 \left(\alpha T_1 + \frac{1}{2} I^2 (R+r/2) - k(T_4 - T_3) - \frac{1}{2} k_{me}(T_4 - T_3) \right) - 2k_w(T_4 - T_0) + 2I^2 r_w = 0 \\
 & \frac{n_1}{2} k_{me}(T_4 - T_5) - k_{c1}(T_4 - T_5) = 0 \\
 & k_{c1}(T_5 - T_6) - \frac{n_2}{2} k_{me}(T_6 - T_7) = 0 \\
 & \dots \\
 & k_{c_{i-1}}(T_{4i-3} - T_{4i-2}) - \frac{n_i}{2} k_{me}(T_{4i-2} - T_{4i-1}) = 0 \\
 & n_i \left(-\alpha T_{4i-1} + \frac{1}{2} I^2 (R+r/2) + k(T_{4i} - T_{4i-1}) + k_{me} \frac{1}{2}(T_{4i-2} - T_{4i-1}) \right) = 0 \\
 & n_i \left(\alpha T_{4i} + \frac{1}{2} I^2 (R+r/2) - k(T_{4i} - T_{4i-1}) - \frac{1}{2} k_{me}(T_{4i} - T_{4i+1}) \right) = 0 \\
 & k_{me} \frac{n_i}{2}(T_{4i} - T_{4i+1}) - k_{c_{i+1}}(T_{4i} - T_{4i+1}) = 0 \\
 & \dots \\
 & k_{c_{N-1}}(T_{4N-3} - T_{4N-2}) - k_{me} \frac{n_N}{2}(T_{4N-2} - T_{4N-1}) = 0 \\
 & n_N \left(-\alpha T_{4N-1} + \frac{1}{2} I^2 (R+r/2) + k(T_{4N} - T_{4N-1}) + k_{me} \frac{1}{2}(T_{4N-2} - T_{4N-1}) \right) = 0 \\
 & n_N \left(\alpha T_{4N} + \frac{1}{2} I^2 (R+r/2) - k(T_{4N} - T_{4N-1}) - \frac{1}{2} k_{me}(T_{4N} - T_{4N+1}) \right) = 0 \\
 & k_{me} \frac{n_N}{2}(T_{4N} - T_{4N+1}) - k_{cN}(T_{4N+1} - T_0) = 0
 \end{aligned} \tag{2.1}$$

The corresponding matrix can be found in Appendix A2.

3. Temperature Dependence of Thermoelectric Material Parameters

In equation (2.1) all the coefficients are considered to be independent of material temperature. However the temperature differential on a TEC must be taken into

account^{5,6}. In a way the picture of temperature distribution can be visualized as in Fig. 3.1.

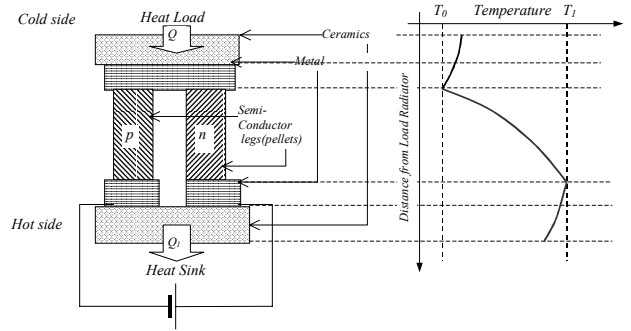


Figure 3.1. A principal view of the temperature differential along a TEC

The picture suggests it be necessary to consider temperature dependence of material parameters. For Bismuth Telluride with commonly used free carriers concentration (about 10^{19} cm^{-3}) these characteristic curves look like those in Fig. 3.2a-c.

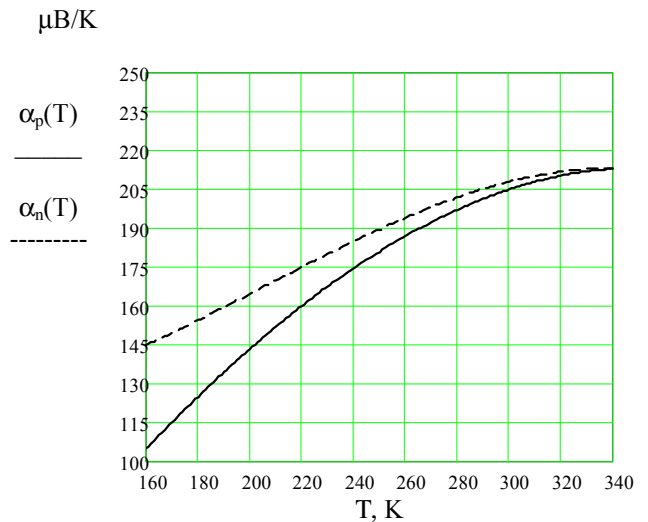


Fig.3.2a. Temperature dependence of Seebeck coefficients for p- and n-types of Bi_2Te_3 (here and in Fig. 3.2b, 3.2c the results¹ are used)

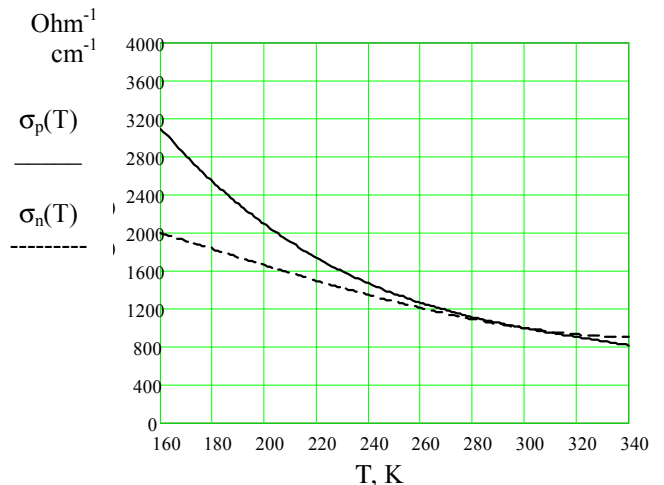


Fig.3.2b. Temperature dependence of electrical conductivities for p- and n-types of Bi₂Te₃

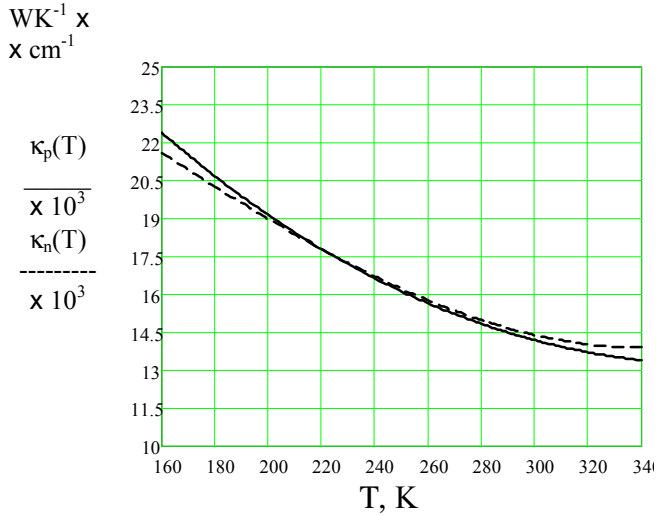


Fig.3.2c. Temperature dependence of thermal conductivities for p- and n-types of Bi₂Te₃

We consider thermal dependences like this. Along each cascade Bi₂Te₃ Seebeck coefficient, thermal and electrical conductivities are taken at the corresponding stage hot side temperature. For example, we consider $\alpha_i(T)$ as $\alpha(T_{i,hot})=const$ at the *i*-th stage. The conciliation of this approach with real parameters gradients and the Thomson effect are given in A3.

The pattern of the modernized matrix A2 for the first stage is transformed in the following way:

$$\begin{matrix} \frac{n_i}{2} \{ \alpha_n(T_i) + \alpha_p(T_i) \} I + k_n(T_i) + k_p(T_i) + k_{me} & n_i \{ k_n(T_i) + k_p(T_i) \} \\ k_n(T_i) + k_p(T_i) & \frac{n_i}{2} \{ \alpha_n(T_i) + \alpha_p(T_i) \} I - k_n(T_i) - k_p(T_i) - k_{me} \end{matrix} \quad (3.1)$$

The added indices refer to the corresponding temperatures. Temperature dependence of electrical resistance in free terms is switched on likewise:

$$\begin{matrix} -Q - k_0 T_0 \\ 0 \\ -\frac{n_i}{2} (R_n(T_i) + R_p(T_i) + r) I^2 \\ -\frac{n_i}{2} (R_n(T_i) + R_p(T_i) + r) I^2 \\ 0 \\ \dots \\ \dots \end{matrix} \quad (3.2)$$

The problem has now become non-linear. However, it can be solved by means of iteration, each time our dealing with the matrix of constant terms.

The algorithm is like this. First we solve the equations set with all the terms at 300K. Then we use the found temperature distribution to specify the term at each level. That yields a new temperature distribution. The procedure is cycled until the necessary accuracy is met.

4. Radiation, Inner Air Losses, Cap Interaction and Heat Sink Finite Thermal Conductance

At the above described iteration we can also take into account radiation and inner air losses. It can be shown that within the simplest assumptions the effective thermal

conductance of the inner part of the TEC should be rewritten as:

$$k' = k (1 + b_{th}), \quad (4.1)$$

where

$$b_{th} = B_{cond} + B_{rad}, \quad (4.2)$$

B_{cond} and B_{rad} are corrections for inter-pellet thermal conductance values through air thermal conductivity and radiation, respectively:

$$B_{cond} = \frac{\kappa_{air}}{\kappa} \left(\frac{l}{\beta} - 1 \right) \quad (4.3)$$

Here the pellets filling term is:

$$\beta = \frac{n_i S}{S_i}, \quad (4.4)$$

where S is the cold side dimensions, n_i is pellets number of a stage;

$$B_{rad} = \gamma \frac{S}{nk} \sigma T_a^3 (1 - \beta) \quad (4.5)$$

where σ is Boltzman constant, γ is thermal emissivity. As for (4.5) it can only be regarded as a rough estimation.

Thus the terms k_i in the program matrix should be modified regarding (4.1) – (4.5).

Taking into account a heat sink (see Fig. 4.1) makes us deal with an additional equation in set (2.1) containing one new unknown temperature on the borderline of the last ceramics and the sink.

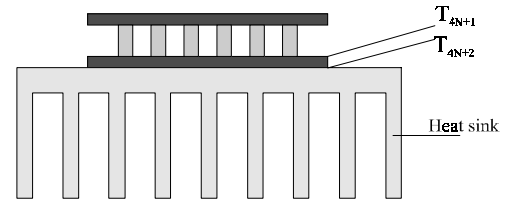


Figure 4.1. A TEC on the heat sink

Here is the relevant equation:

$$k_{cN} (T_{4N+1} - T_{hs}) - K (T_{hs} - T_0) = 0, \quad (4.6)$$

In terms of the matrix (see A2) it is equivalent to the following additional line and changes concerning two last lines:

$$\begin{pmatrix} \dots & \dots & \dots & \dots \\ \dots & \dots & \dots & \dots \\ 0 & \frac{n_N}{2} k_{me} & -\left(\frac{n_N}{2} k_{me} + k_c^N \right) & 0 \\ 0 & 0 & k_c^N & -(k_c^N + K) \end{pmatrix} \begin{pmatrix} \dots \\ \dots \\ T_{4N+1} \\ T_{hs} \end{pmatrix} = \begin{pmatrix} \dots \\ \dots \\ 0 \\ -KT_0 \end{pmatrix} \quad (4.7)$$

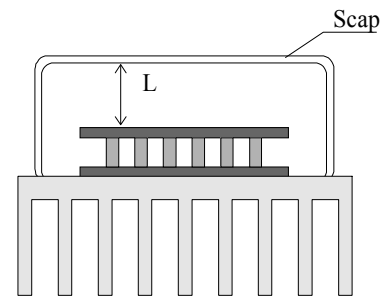


Figure 4.1. A TEC on the heat sink and under the cap

Including cap interaction makes us introduce an effective thermal conductivity K^0 between the upper ceramics (substrate) and the cap inner top:

$$K^0 = \kappa_{air} + \kappa_{conv} + \kappa_{rad}, \quad (4.8)$$

where at normal state and 300K $\kappa_{air} = 0.026 \text{ W/m}\cdot\text{K}$;

$\kappa_{conv} = a \times L [\text{W/m}\cdot\text{K}]$; $a = 4 \text{ W/m}^2 \times \text{K}$ (see Ref.⁷) -

approximate value of the convective heat transfer coefficient

per the surface unit; $\kappa_{rad} = 2\theta \frac{S_c S_{cap} \sigma \bar{T}^3}{\pi L^2}$, θ - surface

emissivity; S_c - the upper ceramic surface, $\sigma = 5.6 \times 10^{-8} \text{ W/m}^2 \text{ K}^4$.

The average temperature \bar{T} is $1/2(T_{hs} + T_0)$ assuming the cup thermal conductance high enough for the cup temperature equal that of the heat sink. The heat amount

$Q_{cap} = K^0 (T_{hs} - T_0)$ should be additional to the active heat load Q (see eqs.(1.1), (2.1)).

5. Standard and Detailed Curves

The approach described above is to be applied to analyzing TEC operation in different modes. Here we present both standard and detailed curves characterizing TEC's in maximum and optimum modes.

These theoretical outputs can be obtained within the all the results discussed here.

5a. Standard Plots

Definitions

Standard curves: the curves, specifying a TEC referred to the maximum delta temperature and maximum heat amount modes

The standard plots involve matrix (A2) directly applying temperature dependence functions (see Fig. 3.2a-c) and corrections (4.1)-(4.4). The standard plots for 2MC10-009-20 are given below.

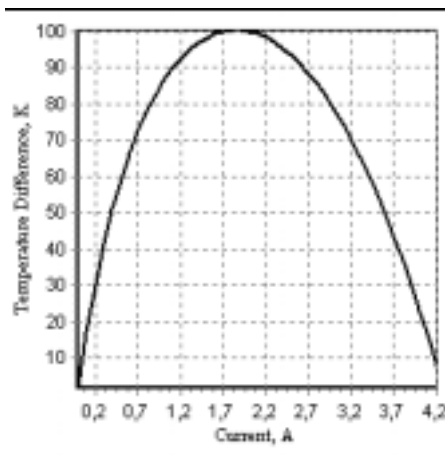


Figure 5a.1. Temperature difference versus device current. Defines ΔT_{max} and I_{max} .

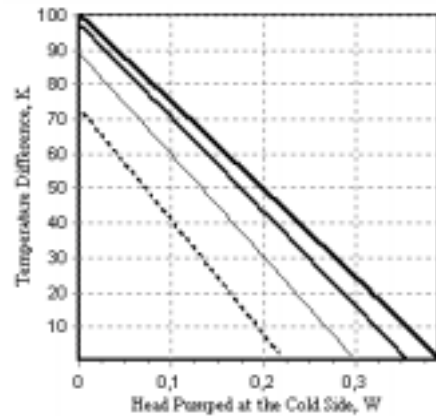


Figure 5a.2. Temperature difference versus heat pumping capacity. Here and further @ (1x, 0.8x, 0.6x, 0.4x) I_{max} ..

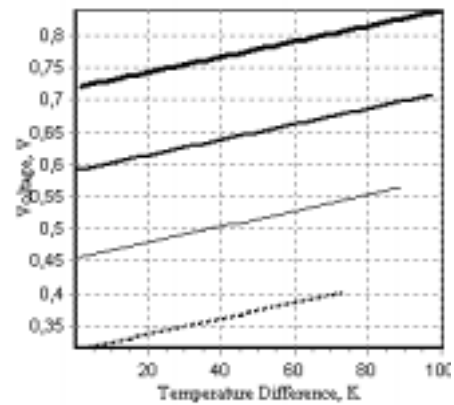


Figure 5a.3. Voltage versus temperature difference.

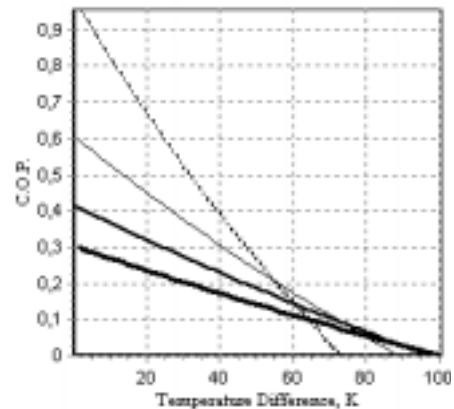


Figure 5a.4. C.O.P. versus temperature difference.

5b. Detailed Plots

Definitions

Detailed curves are the curves, specifying a TEC in the optimal (recommended) mode, i.e., the mode at maximum Coefficient of Performance (C.O.P):

The detailed plots are yielded by a slightly modified matrix. The example of this modification for a 1-stage TEC is presented in (A1.2). The difference from the standard curves case is that the parameter Q is not set a priori and changed step by step until $\Delta T=0$ but is an independent variable whereas ΔT is known and shifted from 0 to ΔT_{max} , the latter defined from the standard plots. Below one can see the detailed plots for 2MC10-009-20.

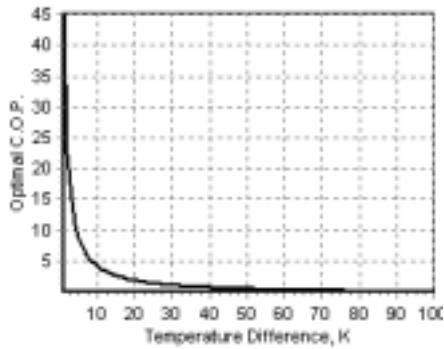


Figure 5b.1. Optimal C.O.P. versus temperature difference

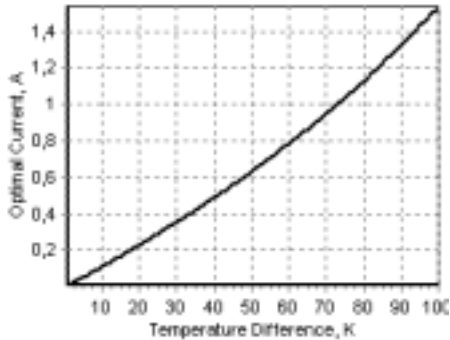


Figure 5b.2. Optimal current versus temperature difference

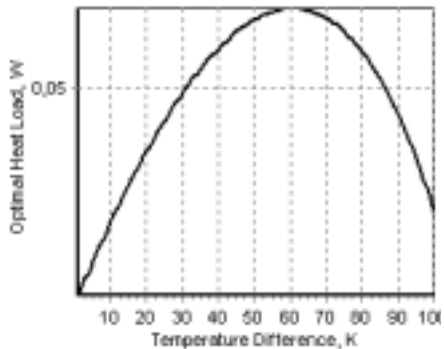


Figure 5b.3. Optimal heat load versus temperature difference

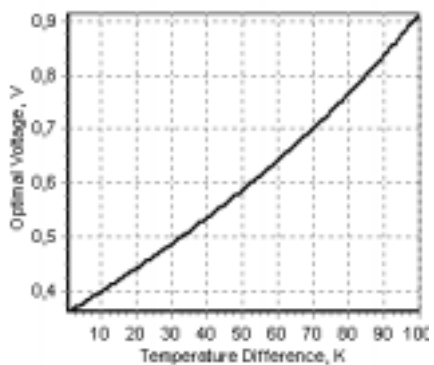


Figure 5b.4. Optimal voltage versus temperature difference

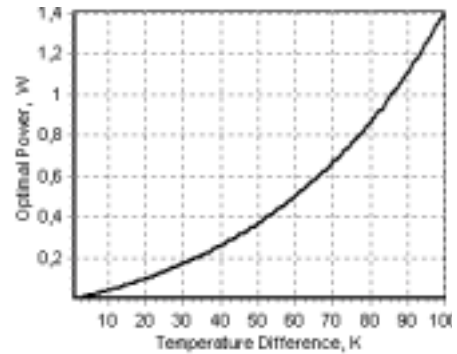


Figure 5b.5. Optimal voltage versus temperature difference

Once the standard plots allow to define extreme limits, the detailed plots give the idea of the most economical TEC operation and recommended cooling mode.

6. Discussion

Armed with this mathematics and graphical support we can solve the problem of reasonable TEC selection and TEC operation optimization with the help of the so-called TECcad program. A User is capable to:

1. obtain standard plots for a TEC and probe it in the maximum mode
2. obtain detailed plots for a TEC and probe it in the optimum mode
3. select an optimal TEC: input desirable cooling parameters (ΔT and Q) or/and electrical and geometrical requirements (cold and hot side areas and height, upper limits of the device current and voltage) and get a TEC or a set of TEC's applicable based on a search cycle in the data bank of TEC's; analyze the selected cooler in operation by visualizing operational curves specifying the selected TEC in maximum and optimal modes;
4. suggest one's own structure, thermoelectric properties and surrounding conditions and analyze the proposed cooler in operation by visualizing operational curves specifying the selected TEC in maximum and optimal modes;
5. examine a TEC in a real housing, that is mounted on a heat sink and under the cap.

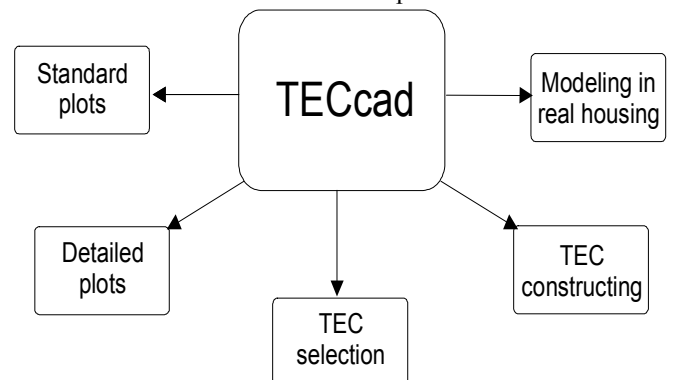


Fig. 6.1. The program TECcad applications.

Figure 6.1 illustrates the above listed options.

Appendixes

A1. One-stage Matrix

$$\begin{pmatrix} -(k_0 + k_{c_0}) & k_{c_0} & 0 & 0 & 0 \\ k_{c_0} & -(k_{c_0} + nk_{me}/2) & nk_{me}/2 & 0 & 0 \\ 0 & nk_{me}/2 & -n(\alpha l + k + k_{me}/2) & nk & 0 \\ 0 & 0 & nk & n(\alpha l - k - k_{me}/2) - k_w & nk_{me}/2 \\ 0 & 0 & 0 & nk_{me}/2 & -(nk_{me}/2 + k_{c_1}) \end{pmatrix} \begin{pmatrix} T_1 \\ T_2 \\ T_3 \\ T_4 \\ T_5 \end{pmatrix} = \begin{pmatrix} -Q - k_0 T_0 \\ 0 \\ -nI^2 (R+r)/2 \\ -nI^2 (R+r)/2 \\ -k_{c_1} T_0 \end{pmatrix} \quad (\text{A1.1})$$

And here is the modification of (A1.1) for the detailed curves problem.

$$\begin{pmatrix} 1 & -(k_0 + k_{c_0}) & k_{c_0} & 0 & 0 & 0 \\ 0 & k_{c_0} & -(k_{c_0} + nk_{me}/2) & nk_{me}/2 & 0 & 0 \\ 0 & 0 & nk_{me}/2 & -n(\alpha l + k + k_{me}/2) & nk & 0 \\ 0 & 0 & 0 & nk & n(\alpha l - k - k_{me}/2) - k_w & nk_{me}/2 \\ 0 & 0 & 0 & 0 & nk_{me}/2 & -(nk_{me}/2 + k_{c_1}) \\ 0 & -1 & 0 & 0 & 0 & 1 \end{pmatrix} \begin{pmatrix} Q \\ T_1 \\ T_2 \\ T_3 \\ T_4 \\ T_5 \end{pmatrix} = \begin{pmatrix} -k_0 T_0 \\ 0 \\ -0.5nI^2 (R+r) \\ -0.5nI^2 (R+r) \\ -k_{c_1} T_0 \\ \Delta \Gamma \end{pmatrix} \quad (\text{A1.2})$$

A2. Multi-stage Matrix

$$\begin{pmatrix} -k_0 - k_{C0} & k_C^0 & 0 & 0 & 0 & 0 & 0 & 0 & 0 & 0 & 0 & 0 \\ k_{C0} & -k_C^0 \frac{n_1}{2} k_{me} & \frac{n_1}{2} k_{me} & 0 & 0 & 0 & 0 & 0 & 0 & 0 & 0 & 0 \\ \dots & \dots & \dots & \dots & \dots & \dots & \dots & \dots & \dots & \dots & \dots & \dots \\ 0 & 0 & 0 & k_C^{i-1} & -k_C^{i-1} \frac{n_i}{2} k_{me} & \frac{n_i}{2} k_{me} & 0 & 0 & 0 & 0 & 0 & 0 \\ 0 & 0 & 0 & 0 & \frac{n_i}{2} k_{me} & -n_i (\alpha l + k + \frac{k_{me}}{2}) & n_i k & 0 & 0 & 0 & 0 & 0 \\ 0 & 0 & 0 & 0 & 0 & n_i k & n_i (\alpha l - k - \frac{k_{me}}{2}) & \frac{n_i}{2} k_{me} & 0 & 0 & 0 & 0 \\ & & & & & & & \frac{n_i}{2} k_{me} & -\frac{n_i}{2} k_{me} - k_C^i & k_C^i & 0 & 0 \\ & & & & & & & \dots & \dots & \dots & \dots & \dots \\ 0 & 0 & 0 & 0 & 0 & 0 & 0 & 0 & 0 & 0 & \frac{n_N}{2} k_{me} & \frac{n_N}{2} k_{me} - k_C^N \end{pmatrix} \begin{pmatrix} T_1 \\ T_2 \\ \dots \\ T_{4i-2} \\ T_{4i-1} \\ T_{4i} \\ T_{4i+1} \\ \dots \\ \dots \\ T_N \\ T_{N+1} \end{pmatrix} = \begin{pmatrix} -Q - k_0 T_0 \\ 0 \\ \dots \\ 0 \\ -\frac{1}{2} n_i I^2 (R+r/2) \\ -\frac{1}{2} n_i I^2 (R+r/2) \\ 0 \\ \dots \\ \dots \\ -\frac{1}{2} n_i I^2 (R+r/2) \\ -k_C^N T_0 \end{pmatrix}$$

A3. Dependence $\alpha(T)$ and Thomson Effect

Let us consider a TEC, indices 0 and 1 identifying the cold and hot sides respectively.

In comparison with^{5,8} we do not take into account the Seebeck coefficient α varying within a leg length. Once we do it, we must consider the Thomson effect as well for the reason that

$$\delta Q_T = I \tau dT, \quad (A3.1)$$

where

$$\tau = T \frac{d\alpha}{dT}, \quad (A3.2)$$

Let us suppose there is α differential along the TEC pellet as depicted at Fig. (A3.1). Therefore the Thomson effect takes place and produces additional cooling as can be viewed by the direction of the Thomson heat flux Q_T in figure A3.1.

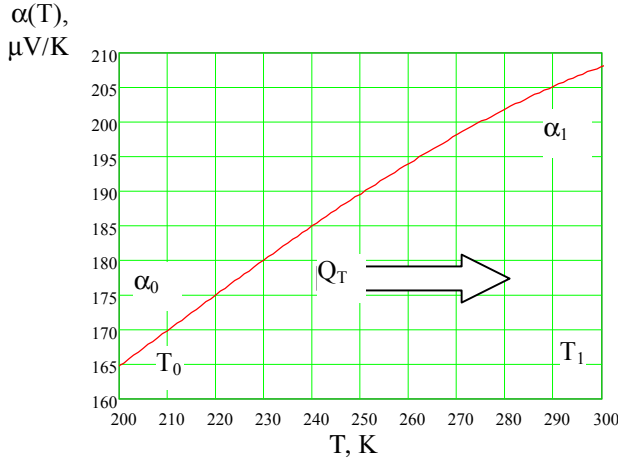


Fig. A3.1. Seebeck coefficient differential and the Thomson effect

As shown in paper⁹ the exact rate equations in this case undergo transformation with all inner heat sources effects being recalculated to the pellets ends and so the material parameters being effective now. For visual aiding we rewrite them⁹ here.

$$\begin{cases} \alpha_{eff 0} IT_0 - \frac{1}{2} I^2 R_{eff 0} - k_{eff 0} \Delta T = Q_0 \\ \alpha_{eff 1} IT_1 + \frac{1}{2} I^2 R_{eff 1} - k_{eff 1} \Delta T = Q_1 \end{cases}, \quad (A3.4)$$

As Drabkin and Dashevsky⁹ go to prove, the effective Z-value specifying ΔT_{max} is defined by the “eff”-parameters of the first equation in (A3.3), that is at the cold side temperature:

$$Z_{eff} = \frac{\alpha_{eff 0}^2}{R_{eff 0} k_{eff 0}}, \quad (A3.4)$$

In the paper considered the exact expressions for $\alpha_{eff 0}$, $R_{eff 0}$, $k_{eff 0}$ are given but here we restrict ourselves just to qualitative explanation.

The Thomson phenomenon is more effective at the cold end of the pellet for $\frac{d\alpha}{dT}$ is higher there, that is

$$\alpha_{eff 0} > \alpha(T_0), \quad (A3.5)$$

As for the effective electrical resistance, it is lower at the pellet cold end (the smaller the temperature value is, the less effective Joule heating takes place), so

$$R_{eff 0} < R, \quad (A3.6)$$

where R - pellet resistance.

The same relation was stressed by Buist⁸. Inequalities (A3.5), (A3.6) were proved by numerical calculation in paper¹⁰. That means the effective figure-of-merit at cold side temperature exceeds a non-effective one at the same temperature, as if shifting all the parameters values to higher temperature. In our work we simplified this by taking all the parameters at the hot side temperature of a stage.

Bibliography

- ¹ L. I. Anatyshuk, *Thermoelements and thermoelectrical devices*//Kiev, 1979.
- ² H.J.Goldsmid, *Electronic Refrigeration*// Pion Ltd, 1986
- ³ V.A. Semeniouk, T.V.Pilepenko, *Thermoelectric Cooling of Semiconductor Lasers under Extreme Temperature Conditions*// Proceedings of the XIV Int. Conf. On Thermoelectrics, St. Petersburg, Russia, 1995, p. 469-473
- ⁴ Vayner A.L., *Thermoelectric coolers*// Moscow, 1983.
- ⁵ Paul G.Lau and Richard J.Buist, *Calculation of Thermoelectric Power Generation Performance Using Finite Element Analysis*// Proceedings of the 16th International Conference on Thermoelectrics (1997).
- ⁶ M.H. Cobble *Calculations of Generator Performance*// CRC Handbook of Thermoelectrics, CRC Press, Inc., 1995.
- ⁷ Dulnev G.N. *Thermal exchange in the radioelectrical devices*//Leningrad, 1963, p. 14-20.
- ⁸ R. Buist. *The extrinsic Thomson effect*. //Proceedings of the XIV Int. Conf. On Thermoelectrics, St. Petersburg, Russia, 1995, p.301-304.
- ⁹ Drabkin I.A., Dashevsky Z.M., *Basic Energy Relations for Cooler Die Taking into Account Temperature Dependence of Thermoelectric Parameters*// Proceedings of the 7th Interstate Seminar, S.-Petersburg, 2000, p.292-297
- ¹⁰ Drabkin I.A, *Difference in Operation of p- and n-Type Cooling Dice with Thermoelectric Materials based on Bi₂Te₃*// Proceedings of the 7th Interstate Seminar, S.-Petersburg, 2000, p.298-302